Reprinted from:

Nuclear Physics **A362** (1981) 137–162;

MULTI-STEP SHELL-MODEL TREATMENT OF SIX-PARTICLE SYSTEMS

R. J. LIOTTA †

Laboratoire de Physique Théorique ‡, Université de Bordeaux I, Chemin du Solarium, 33170 Gradignan, Fran

and

Centre d'Etudes Nucléaires de Bordeaux-Gradignan ‡, Domaine du Haut-Vigneau, 33170 Gradignan, Fran

and

NORTH HOLLAND

AMSTERDAM

Nuclear Physics **A362** (1981) 137–162;

MULTI-STEP SHELL-MODEL TREATMENT OF SIX-PARTICLE SYSTEMS

R. J. LIOTTA †

Laboratoire de Physique Théorique ‡, Université de Bordeaux I, Chemin du Solarium, 33170 Gradignan, France
and
Centre d'Etudes Nucléaires de Bordeaux-Gradignan ‡, Domaine du Haut-Vigneau, 33170 Gradignan, France

and

C. POMAR

Departamento de Fisica, CNEA, Av. del Libertador 8250, 1429 Buenos Aires, Argentina

Received 13 October 1980

Abstract: A method is presented of solving the six-particle systems in several steps. In the first step, the two-particle spectrum is calculated within the standard shell model. In the second step, the four-particle system is solved within a (correlated) basis consisting of the vector-coupled two-particle states previously evaluated. Finally, in the third step the six-particle system is calculated using a basis formed by vector coupling the two- and four-particle spectra evaluated in the first two steps. The method is applied to analyse the spectra and (p, t) reactions leading to ^{204}Pb and ^{202}Pb and good agreement with experimental data is obtained. A liaison between this calculation and the pairing model is found and the importance of the Pauli principle upon the pairing vibrational states is attested.

1. Introduction

The shell model has been very successful in explaining the structure of nuclei close to spherical cores. But if the number of valence particles becomes large enough the application of the shell model is a burdensome task even for the mighty computers of today. This is due essentially to the fact that the standard shell model is not suited to make further truncations to the shell-model basis [14]) (which already spans only a small subspace of the total Hilbert space). For this reason, several methods and models have been proposed which allow one to carry on additional truncations [1–8]). A common feature of these methods is that they already contain the two-particle correlations in the basis that induce the collectivity of the low-spin yrast states. Thus, the spreading of the shell-model wave function into a large number of equally important components is avoided. Moreover, the physical vectors are often contained in a relatively small subspace of the total space spanned

† On leave from Research Institute for Physics, Stockholm, Sweden.
‡ Equipe de Recherche Associée au CNRS.

by the correlated basis so that the calculation and interpretation of the wave functions are rather easy to perform.

In spite of these advantages, those methods also face computational problems when the number of valence particles becomes large. Already for the four-particle system the formalism may not be easy to handle [3,4]). In addition to the dynamical matrix one has also generally to evaluate the overlap matrix among the basis vectors, the so-called metric matrix (however, as an exception, in the nuclear field theory [7]) one does not need to evaluate the metric matrix directly). Finally, in some cases spurious states appear which can mix with the physical states [5,6,8]).

The necessity of evaluating both the dynamical and overlap matrices may make the application of the formalism rather cumbersome. An important step to simplify the formalism was given in ref. [5]) where the bare two-particle interaction was replaced by the corresponding correlated energies and wave functions. It was later realized that within this formalism the metric matrix is essentially the same as the dynamical matrix in some cases [9]). Recently it was proposed to extend the method of ref. [9]), which dealt only with systems with three particles outside the core, to more complex situations [11]). It was thus found that for the four-particle system the property that the metric matrix is essentially the same as the dynamical matrix holds. For the six-particle system, analysed in term of the two- and four-particle systems, that property is not found but still the final equations turned out to be simple and the method rather effective. Perhaps the most important point in ref. [11]) is that the six-particle system is solved in several steps. First the two-particle system [which defines the two-particle interaction [5])] is solved. With the two-particle energies and wave functions one solves the four-particle system [thus the "two-step shell model" of Ma and True [4])]. With the two- and four-particle systems already evaluated one goes forward to calculate the six-particle system.

Together with the many methods invented in order to profit by the two-particle correlations that are present in correlated basis, a number of names have been introduced for those methods. We find that the name given by Ma and True [4]) represents well what is behind the method presented here, and have adopted to call our procedure the "multi-step shell-model method".

In this paper we present in detail the multi-step shell-model method for the case of six-particle systems outside closed-shell cores and apply it to the lead region. The formalism is given in sect. 2. In sect. 3 we study the ^{204}Pb and ^{202}Pb spectra, and our conclusions are in sect. 4.

2. Formalism

2.1. DYNAMICAL EQUATIONS

A system with two particles outside a closed-shell core is described within the shell-model representation, in principle, by means of an unlimited number of

particle-hole excitations on top of the two-particle excitations. The great advantage of the shell-model basis lies precisely in the fact that in practice only very few of those excitations are needed to have a good description of the experimental data. In the limiting case when all particle-hole excitations are neglected one gets the so-called Tamm-Dancoff approximation (TDA). In this case the total set of coupled shell-model equations reduces to

$$(\omega_\alpha - \varepsilon_i - \varepsilon_j) X(ij;\alpha) = \sum_{k \leqq l} \langle kl;\alpha|V|ij;\alpha\rangle\, X(kl;\alpha), \tag{1a}$$

where

$$X(ij;\alpha) = \langle\alpha|(C_i^\dagger C_j^\dagger)_\alpha|0\rangle/(1+\delta_{ij})^{\frac{1}{2}}. \tag{1b}$$

In eq. (1) and throughout this paper the index α labels two-particle states and the indices i, j, k, l label single-particle states. In all cases we use the same symbols to label states as well as the corresponding angular momenta as seen, for instance, in the nine-j symbol of eq. (5b). As usual, $\omega(\varepsilon)$ indicates the two-particle (single-particle) energy and $C^\dagger$ the fermion creation operator. The diagonalization of the matrix (1a) provides the TDA wave function

$$|\alpha\rangle = P^\dagger(\alpha)|0\rangle, \tag{2}$$

where

$$P^\dagger(\alpha) = \sum_{i \leqq j} X(ij;\alpha)(C_i^\dagger C_j^\dagger)_\alpha/(1+\delta_{ij})^{\frac{1}{2}} \tag{3}$$

is the two-particle creation operator.

Eq. (3) allows us to write

$$(C_i^\dagger C_j^\dagger)_\alpha/(1+\delta_{ij})^{\frac{1}{2}} = \sum_\alpha X^*(ij;\alpha) P^\dagger(\alpha). \tag{4}$$

The TDA equations for the four-particle system outside a closed-shell core contain the matrix elements of the two-particle interaction in combinations that can also be written, using eq. (4), in the form (1a), as was first realized in refs. [5,6]). One then obtains †

$$(W_\beta - \omega_{\alpha_1} - \omega_{\alpha_2})\langle\beta|(P^\dagger(\alpha_1)P^\dagger(\alpha_2))_\beta|0\rangle$$
$$= -\sum_{\alpha_3\alpha_4}\sum_{ijkl} (\omega_{\alpha_3} - \varepsilon_j - \varepsilon_k) A(ijkl;\alpha_1\alpha_2\alpha_3\alpha_4)\langle\beta|(P^\dagger(\alpha_3)P^\dagger(\alpha_4))_\beta|0\rangle, \tag{5a}$$

where

$$A(ijkl;\alpha_1\alpha_2\alpha_3\alpha_4) = Y(ij;\alpha_1)Y(kl;\alpha_2) \times Y^*(ik;\alpha_3)Y^*(jl;\alpha_4)\hat{\alpha}_1\hat{\alpha}_2\hat{\alpha}_3\hat{\alpha}_4 \begin{Bmatrix} i & j & \alpha_1 \\ k & l & \alpha_2 \\ \alpha_3 & \alpha_4 & \beta \end{Bmatrix}. \tag{5b}$$

† A brief presentation of the present paper was given in a recent letter [11]). However a number of typing errors have slipped into the equations of that letter.

We use the index β to label four-particle states with the corresponding four-particle energies W_β, while

$$Y(ij;\alpha) = (1+\delta_{ij})^{\frac{1}{2}} X(ij;\alpha).$$

It is worthwhile to point out that to obtain eq. (5) we assumed that the four-particle system was decomposed into two blocks. Each block is the two-particle system [2-6]), but one can also obtain a similar equation assuming one of the blocks to be composed of the one-particle and the other of the three-particle systems. In the same fashion, we describe below the six-particle system in terms of the two- and four-particle systems but any other partition can be chosen just as well. We chose the partitions mentioned above because we have in mind to analyse the (p, t) experimental data of ref. [12]) for which our choice seems natural.

In eq. (5) the matrix elements of the two-particle interaction have been replaced by the two-particle energies and wave functions. Although this property is not, in principle, an advantage (since the knowledge of one thing implies the knowledge of the other), the formalism itself has become rather simple as can be seen by comparing eq. (5) with the corresponding equations in refs. [3,4]). Moreover, in some cases it might be possible to use in eq. (5) only a few two-particle states: precisely those for which both the energy and wave-function amplitudes are experimentally known. In particular, this is true for the $N = 50$ isotones as shown in sect. 3.

Eq. (5) provides a simple and elegant framework in which to analyse four-particle excitations. It is even tempting to assume that the diagonalization of eq. (5) with the usual normalization condition for the amplitudes (i.e. the sum of the squares equal to one) provides both the energies and wave functions of the four-particle states [6]). This procedure, however, is equivalent to assuming that the basis vectors

$$\{|\alpha_1\alpha_2;\beta\rangle\} = \{(P^\dagger(\alpha_1)P^\dagger(\alpha_2))^\dagger_\beta|0\rangle\} \tag{6}$$

form an orthogonal basis, which is generally not true. Nevertheless the set of energies provided by such a diagonalization contains the shell-model energies if all possible basis states are included [6]). Yet, since the Pauli principle is not acting in eq. (6) between the fermions in $P^\dagger(\alpha_1)$ and the fermions in $P^\dagger(\alpha_2)$, the dimension of the matrix (5) is larger than the corresponding shell-model dimension. One thus obtains a number of spurious solutions, in addition to the physical solutions, by direct diagonalization of the matrix (5). The spurious roots can rather easily be disentangled from the physical roots if all possible basis elements (6) are included [6]). However, in practice the basis is strongly truncated and mixing among the spurious and physical roots might become important.

Another drawback of the matrix (5) is that it is not hermitian and therefore complex solutions may be encountered.

To overcome these problems one can evaluate the overlap matrix among the basis states [3,5,9]) (metric matrix). One can then utilize any of the available methods to construct an orthonormal basis. But this procedure may spoil the simplicity of

the formalism if the metric matrix is difficult to calculate. However, an important point of ref. [9]) was that the metric and the dynamical matrices were very similar in some cases. For the four-particle system analysed here one obtains

$$\langle 0|(P^{\dagger}(\alpha_1)P^{\dagger}(\alpha_2))^{\dagger}_{\beta}(P^{\dagger}(\alpha_3)P^{\dagger}(\alpha_4))_{\beta}|0\rangle = \delta_{\alpha_1\alpha_3}\delta_{\alpha_2\alpha_4} + (-1)^{\alpha_1+\alpha_2-\beta}\delta_{\alpha_1\alpha_4}\delta_{\alpha_2\alpha_3} - \sum_{ijkl} A(ijkl;\, \alpha_1\alpha_2\alpha_3\alpha_4), \tag{7}$$

which can be evaluated at the same time as (5a).

Making use of the metric matrix one can transform the non-hermitian matrix (5a) into a hermitian matrix T (which has the right dimensions) if all possible basis states (6) are included. Following ref. [9]) we write the hermitian matrix T as

$$T(m, m') = \lambda_{m'} \sum_{bb'} \xi_m(b) M(b, b') \xi^*_{m'}(b'), \tag{8a}$$

where M is the matrix (5a), and λ and ξ are the eigenvalues and eigenvectors, respectively, of the metric matrix (7). The letter b labels the non-orthogonal basis elements (6) and m labels the orthonormal basis elements resulting from the diagonalization of the metric matrix.

In deriving eq. (8a) it was supposed that all possible basis elements b (constructed from the original single-particle states) were included. However, we expect to be able to drastically truncate the dimensions of the original space without much affecting the description of the physical vectors. When this truncation is done only a small number of elements b enter in eq. (8a) and the matrix T may loose its hermiticity. This property may tell us how far have we gone with the truncation. If the calculated matrix T, which we call T_c, is still approximately hermitian in the truncated space one can assume that the truncation procedure has been correct. Moreover, in this case one can proceed with the calculation utilizing the matrix

$$\tilde{T} = \tfrac{1}{2}(T_c + T_c^{\dagger}), \tag{8b}$$

instead of the non-hermitian matrix T_c. We use this procedure throughout this paper. Specific details will be given in sect. 3. Here we want to observe that even if the space spanned by the truncated set of vectors $\{b\}$ contains the physical vector $|n\rangle$, the diagonalization of the corresponding matrix $\tilde{T}$ may not provide a good description of $|n\rangle$. This is due to the fact that the vector $|n\rangle$ may have large projections onto basis vectors outside the set $\{b\}$. This feature will be important in understanding some of the results in the applications given in sect. 3.

The diagonalization of $\tilde{T}$ provides the physical four-particle states, i.e.

$$|\beta\rangle = P^{\dagger}(\beta)|0\rangle, \tag{9a}$$

where

$$P^{\dagger}(\beta) = \sum_{\alpha_1 \leqq \alpha_2} X(\alpha_1\alpha_2;\, \beta)(P^{\dagger}(\alpha_1)P^{\dagger}(\alpha_2))_{\beta}. \tag{9b}$$

We use the same symbols in eq. (9) as in eqs. (3) and (14) for the wave-function amplitudes and the creation operators $P^\dagger$. However, no confusion can arise since the labels clearly identify the various quantities.

Since the coordinates of a vector in an overcomplete basis are not well-defined quantities, the amplitudes X in eq. (9) are not well defined either. But the quantity

$$F(\alpha_1\alpha_2;\beta) = \langle\beta|(P^\dagger(\alpha_1)P^\dagger(\alpha_2))_\beta|0\rangle, \tag{10}$$

which is closely related to the two-particle transfer form factor (see subsect. 2.2), does not depend upon the basis used. It simply represents the projection of the physical vector $|\beta\rangle$ onto the basis vector (6). For the two-particle system the quantity equivalent to F is the complex conjugate of the two-particle amplitude X [eq.(3)]. That simple relation does not hold when the basis elements are not orthogonal to each other. But one still obtains, from eq. (9),

$$\sum_{\alpha_1 \leqq \alpha_2} X(\alpha_1\alpha_2;\beta_1)F(\alpha_1\alpha_2;\beta_2) = \delta_{\beta_1\beta_2}.$$

It is worthwhile to point out that the quantity F is a by-product of our calculation.

For the six-particle system one can proceed as for the four-particle case. One writes down the six-particle TDA equation to find that this equation can be expressed in terms of the two- and four-particle TDA energies and wave-function amplitudes. One gets

$$(W_\gamma - W_{\beta_1} - \omega_{\alpha_1})\langle\gamma|(P^\dagger(\alpha_1)P^\dagger(\beta_1))_\gamma|0\rangle = \sum_{\alpha_2\beta_2}\sum_{\alpha_3}(W_{\beta_2} - \omega_{\alpha_1} - \omega_{\alpha_3})Y(\alpha_3\alpha_2;\beta_1)$$

$$\times F^*(\alpha_3\alpha_1;\beta_2)\hat{\beta}_1\hat{\beta}_2 \begin{Bmatrix} \alpha_1 & \alpha_3 & \beta_2 \\ \alpha_2 & \gamma & \beta_1 \end{Bmatrix} \langle\gamma|(P^\dagger(\alpha_2)P^\dagger(\beta_2))_\gamma|0\rangle, \tag{11}$$

where we use the letter γ to label the six-particle state with energy W_γ, while $Y(\alpha_1\alpha_2;\beta) = (1+\delta_{\alpha_1\alpha_2})X(\alpha_1\alpha_2;\beta)$ and F is from eq. (10).

The six-particle equation (11) depends only upon two- and four-particle quantities. Thus, once the four-particle system has been solved one can proceed further to evaluate eq. (11). This equation presents the same drawbacks as the corresponding equation for the four-particle system (5), but it also presents the same advantages. On the one hand, eq. (11) is not hermitian and its direct diagonalization is not very meaningful because the basis elements $(P^\dagger(\alpha)P^\dagger(\beta))_\gamma|0\rangle$ are not orthogonal to each other. Since the matrix (11) does not fully reflect the Pauli principle its dimension N is larger than the physical dimension n. It therefore must also give a number $N-n$ of spurious roots. On the other hand, it is somehow surprising to find that the six-particle equation (11) is even simpler than the corresponding equation (5) for the four-particle system. It would thus seem that, within this formalism, once the four-particle energies and wave functions are calculated one can go to the next step and solve the six-particle system straightforwardly. This is unfortunately not completely true because, as before, one must calculate the metric matrix which, after

some algebra, can be written as

$$\langle 0|(P^\dagger(\alpha_1)P^\dagger(\beta_1))^\dagger_\gamma(P^\dagger(\alpha_2)P^\dagger(\beta_2))_\gamma|0\rangle = \delta_{\alpha_1\alpha_2}\delta_{\beta_1\beta_2}+\sum_{\alpha_3}F(\alpha_3\alpha_2;\beta_1)$$
$$\times F^*(\alpha_3\alpha_1;\beta_2)\hat{\beta}_1\hat{\beta}_2\begin{Bmatrix}\alpha_1 & \alpha_3 & \beta_2\\ \alpha_2 & \gamma & \beta_1\end{Bmatrix}+\sum_{\alpha_3\alpha_4\alpha_5}\sum_{\beta}Y(\alpha_4\alpha_3;\beta_2)F(\alpha_5\alpha_3;\beta_1)$$
$$\times D(\alpha_5\alpha_1,\alpha_4\alpha_2;\beta)\hat{\beta}_1\hat{\beta}_2\hat{\beta}^2\begin{Bmatrix}\alpha_3 & \alpha_4 & \beta_2\\ \alpha_2 & \gamma & \beta\end{Bmatrix}\begin{Bmatrix}\alpha_3 & \alpha_5 & \beta_1\\ \alpha_1 & \gamma & \beta\end{Bmatrix}, \tag{12}$$

where D is related to the four-particle metric (7) as

$$D(\alpha_1\alpha_2,\alpha_3\alpha_4;\beta) = \langle 0|(P^\dagger(\alpha_1)P^\dagger(\alpha_2))^\dagger_\beta(P^\dagger(\alpha_3)P^\dagger(\alpha_4))_\beta|0\rangle$$
$$-\delta_{\alpha_1\alpha_3}\delta_{\alpha_2\alpha_4}-(-1)^{\alpha_1+\alpha_2-\beta}\delta_{\alpha_1\alpha_4}\delta_{\alpha_2\alpha_3}. \tag{13}$$

The quantity D would be zero if the operators $P^\dagger(\alpha)$ were boson creation operators, i.e. if the Pauli principle were not effective. In this case the last term in eq. (12) would vanish and eq. (12) would be as similar to eq. (11) as eq. (7) is to eq. (5). Thus, if the approximation of considering the two-particle creation operators as boson operators in the intermediate states of eq. (12) is valid, the six-particle system would indeed be as easy to solve as the three-particle system was. Actually, within this approximation the six-particle equations (11) and (12) are formally identical to the corresponding three-particle equations [9]). In sect. 3 we will analyse how good this "quasi-boson" approximation of setting $D = 0$ in eq. (12) is.

With the aid of the metric matrix (12) one can then evaluate the six-particle wave function as

$$|\gamma\rangle = P^\dagger(\gamma)|0\rangle, \tag{14a}$$

where

$$P^\dagger(\gamma) = \sum_{\alpha\beta}X(\alpha\beta;\gamma)(P^\dagger(\alpha)P^\dagger(\beta))_\gamma. \tag{14b}$$

As for the four-particle case, eq. (11) with the constraint imposed by the metric (12) leads to an hermitian matrix T [eq. (8a)]. Again here this matrix has the right dimensions, i.e. no spurious states are present, and one gets the same results as those provided by the shell model if no truncation is made. But the truncation procedure may cause the loss of that hermiticity leading to a non-hermitian matrix T_c. As before, if the matrix T_c is still approximately hermitian we assume that the truncation procedure has been correct. We then define the hermitian matrix $\tilde{T}$ [eq. (8b)], which is supposed to provide, approximately, the shell-model states, as discussed in set. 3.

Defining

$$F(\alpha\beta;\gamma) = \langle\gamma|(P^\dagger(\alpha)P^\dagger(\beta))_\gamma|0\rangle, \tag{15}$$

which is the equivalent to the four-particle quantity (10), the normalization condition

for the six-particle wave function becomes

$$\sum_{\alpha\beta} X(\alpha\beta;\gamma_1)F(\alpha\beta;\gamma_2) = \delta_{\gamma_1\gamma_2}. \tag{16}$$

As for the four-particle case, F is closely related to the two-particle transfer form factor (see below). Also here F is a by-product of the calculation.

2.2. TWO-PARTICLE TRANSFER FORM FACTORS

Two-particle transfer reactions are of great importance in probing pairing correlations [16]. In fact, the "collectivity" of a state with respect to particle-particle correlations is seen well in this type of reactions because for the "collective" states all components of the wave functions contribute in phase. One thus obtains great enhancements relative to pure configuration hmits [17]. It would thus be quite interesting to analyse two-particle transfer reactions in the lead region, where normal pairing phonons are known to play an important role [18,35-37].

The dependence of the two-particle transfer reaction on the nuclear structure is described by the form factor.

Assuming the target nucleus to be in the ground state and the residual nucleus to be in the excited state, $|n\rangle$ (with angular momentum λ_n), the two-particle form factor is defined as [19]

$$f(ij;n) = \langle n|(C_i^\dagger C_j^\dagger)_{\lambda_n}|\text{g.s.}\rangle/(1+\delta_{ij})^{\frac{1}{2}}, \tag{17}$$

which coincides with the two-particle amplitude X^* [eq. (3)] if the target is the core.

In our formalism the form factor (17) may better be rewritten, using eq. (4), as

$$f(ij;n) = \sum_\alpha X^*(ij;\alpha)\,\langle n|P^\dagger(\alpha)|\text{g.s.}\rangle, \tag{18}$$

this expression is just tailored to be evaluated through the equations derived in the previous subsection. In fact, if $|n\rangle$ is one of the four-particle states (9) one gets, from eq. (10),

$$f(ij;\beta) = \sum_\alpha X^*(ij;\alpha)F(\alpha\alpha_0;\beta), \tag{19}$$

where α_0 labels the ground state of the two-particle system. In the same fashion, if $|n\rangle$ is one of the six-particle states (14) one obtains

$$f(ij;\gamma) = \sum_\alpha X^*(ij;\alpha)F(\alpha\beta_0;\gamma), \tag{20}$$

where $|\beta_0\rangle$ is the four-particle ground state and F is from eq. (15).

Although the calculation of the form factors (19) and (20) is straightforward there is the inconvenience in that all non-negligible values of F must be known. Some of the intermediate states in (19) and (20) may not belong to the basis used to describe the physical vector. Therefore (and since these vectors are in general not

orthogonal to each other) large values of F may exist which have not been calculated through the diagonalization of $\tilde{T}$. To circumvent this problem one may follow one of the following two procedures:

(a) To include all intermediate states in the basis, even when they are not necessary to describe the physical vector. Notice that the presence of α_0 (or β_0) in (19) [or (20)] greatly reduces the number of those intermediate vectors.

(b) To evaluate F for the intermediate states which do not belong to the basis expanding the physical vector in (10) or (15) according to (9) or (14). For the six-particle case of eq. (20) one obtains

$$F(\alpha\beta_0;\gamma) = \sum_{\alpha_1\beta_1} X(\alpha_1\beta_1;\gamma)\,\langle 0|(P^\dagger(\alpha_1)P^\dagger(\beta_1))^\dagger_\gamma (P^\dagger(\alpha)P^\dagger(\beta_0))_\gamma|0\rangle, \tag{21}$$

and a similar expression for the function F in (19). The overlap matrix element in the r.h.s. of eq. (21) can be calculated independently of the physical vector. In particular, using eq. (7) the form factor (19) becomes

$$f(ij;\beta) = \sum_\alpha X^*(ij;\alpha)Y^*(\alpha\alpha_0;\beta) + (1+\delta_{ij})^{-\frac{1}{2}} \sum_{\alpha_1\alpha_2} \hat{\alpha}_1\hat{\alpha}_2 Y^*(\alpha_1\alpha_2;\beta)$$

$$\times \sum_k \hat{k}^{-1} \begin{Bmatrix} \alpha_1 & \alpha_2 & \beta \\ i & j & k \end{Bmatrix} Y^*(ki;\alpha_2)Y(kk;\alpha_0)Y^*(jk;\alpha_1). \tag{23}$$

In the following section we use the two procedures outlined above to analyse the ^{206,204}Pb(p, t) cross sections.

3. Applications

In the method presented in the previous section a good description of a system with a given number of particles is needed to calculate more complex systems. In each step one constructs a building block to be used in the following step. This idea is behind all methods and models that use correlated states in the basis. In a sense, the shell model itself is built upon this underlying idea, when assuming that the experimental single-particle levels correspond to the Hartree-Fock representation. Another important feature of the shell model is that in taking only the lowest states of each spin and parity in the odd system close to the core, one assumes that the states of the nuclei beyond are not influenced by high-lying single-particle states. There are cases, like the formation of the α-particle in α-decay [20], where a large number of single-particle levels are necessary. But usually one does not need to include more than a major shell to describe the low-lying states of nuclei with a few valence nucleons outside the core. A striking example is the region around ^{88}Sr, where $Z = 38$ is considered to be a magic number. Including only two single-particle orbits one gets a good description of the low-lying levels of the $N = 50$ isotones [15]. Moreover, it was recently found in the same region that even the defor-

mation that sets in around $Z = 40$, $N = 60$ can be explained within a small shell-model subspace [21]) [see also ref. [22])].

Therefore, it seems that it is reasonable within our method to assume that only the lowest states of the two-particle system are important to describe the low-lying levels in the four-particle system, as we do below. In the same fashion, we assume that only the lowest levels in the two- and four-particle systems are important to describe the six-particle system.

This energy criterion underlies our whole method. In the applications below, however, we will see that in some cases (especially in ^{202}Pb) even more restrictive conditions will be enough to have a good description of the physical vectors.

An important question is how well one must calculate a system to go forward in the calculation of the next system. It would be a serious drawback if the errors that inevitably are committed when truncating the basis are propagated very fast. To avoid as much as possible this problem we "renormalize" the energies of the states calculated in a given step to the experimental values. As mentioned above, this is done with the shell-model single-particle states and in some of the methods that use a correlated basis with the two-particle states [25]).

Another feature that one might have to consider is the effect of the number of valence particles upon the active orbits [23,24]). We neglect this effect because it may not be so important in the lead region, where the number of valence particle cannot be very large with respect to the number of core particles.

To check the formalism (and our computer code) we applied it to the $Z = 38$ region mentioned above. Since there are only two single-particle levels, an exact calculation is readily feasible. All two-particle states are experimentally known (the wave functions through stripping reactions on the ^{90}Zr target). Therefore, in this case one can calculate the four-particle spectrum (the nucleus ^{92}Mo) directly from eq. (5) without passing through the two-particle interaction.

Our calculations agree with the shell-model calculations reported in ref. [15]). But our main purpose is to analyse the ^{204}Pb and ^{202}Pb spectra and (p, t) reactions [12]) for which, as mentioned in the previous section, normal pairing vibrations should play an important role. The number of single-particle states to be considered in this case is large enough to make a standard shell-model calculation nearly impossible. However, McGrory and Kuo calculated (within the shell model) the 0^+, 2^+ and 4^+ states in ^{204}Pb, obtaining good agreement with experimental data [27]). The (p, t) experimental data have also been partially analysed in refs. [33,36]).

Perhaps the most impressive shell-model calculations in the lead region are those by Blomqvist, who predicted a large number of yrast states (both energies and lifetimes) with remarkable accuracy [28-30]). In these calculations it was generally assumed that very few configurations were relevant for each (high) spin. This shows that the standard shell-model is well suited to study nuclei with several valence particles in this region.

3.1. α-STATES: THE NUCLEUS ^{206}Pb

Once the single-particle levels are determined, the first step in our procedure is to calculate the two-particle states, or α-states, as they were called in sect. 2. To make this calculation one needs to know the nucleon-nucleon interaction or else find a way to evaluate the two-body matrix elements [15,26]. We took the ^{206}Pb wave functions and energies from the calculation by Blomqvist [31]. The shell-model space is determined by the single-particle levels shown in table 1. The matrix

TABLE 1

Single-particle states used in the calculations

i	$2p_{1/2}$	$1f_{5/2}$	$2p_{3/2}$	$0i_{13/2}$	$1f_{7/2}$	$0h_{9/2}$
ε_i	7.368	7.938	8.266	9.001	9.708	10.768

Energies are in MeV.

elements of the interaction were calculated by Blomqvist using the theoretical matrix elements of the approximation 2 of Kuo and Herling [32] (i.e. bare interaction plus the "bubble" contribution) which already gives a good description of ^{206}Pb. Some of those matrix elements were changed empirically to obtain an excellent fitting of the experimental data [cf. table 1 of ref. [30]]. With these wave functions we calculated the ^{208}Pb(p, t) cross sections, as shown in table 2. Considering the ambiguities inherent to the DWBA for the two-particle transfer case [17] one can well say that the agreement between theory and experiment is good. At the same time, since the results of table 2 correspond to the first building block of our method we can not expect to have, in what follows, better results than those in table 2.

3.2. β-STATES: THE NUCLEUS ^{204}Pb

The second step in our method is to calculate the four-particle states, i.e. the β-states of sect. 2. In order to make the presentation clear we call the set of basis elements (6) used to perform the calculation the "β-basis".

We first choose a large β-basis to have a description of the β-states as close as possible to the corresponding shell-model description. We thus took the first 25 lowest α-states to form a rather large set of basis elements (6). From this set we selected the first 50 elements (with lowest zero-order energy). To form the β-basis we finally added to those 50 elements all the intermediate states $|\alpha\alpha_0; \beta\rangle$ in (19), which were not present in the 50 element set. The dimension of the β-basis thus built was always less than 60.

Within this β-basis we applied eqs. (5) and (7) to calculate the matrix T_c and the hermitian matrix $\tilde{T}$ [eq. (8b)]. This "large" β-basis spans in fact a small subspace

TABLE 2

Experimental [40]) and calculated [31]) ^{206}Pb spectrum

J^π_α	Experiment		Theory	
	E	σ_{rel}	E	σ_{rel}
0^+_1	0	1	0	1
0^+_2	1.167	0.099	1.167	0.029
0^+_3	2.314	0.174	2.314	0.27
2^+_1	0.804	1	0.803	1
2^+_2	1.466	0.151	1.466	0.19
2^+_3	1.783	0.014	1.783	0.0029
2^+_4	2.147	0.081	2.147	0.025
2^+_5	2.421	0.098	2.421	0.13
2^+_6			3.223	0.017
2^+_7			3.533	0.038
2^+_8	3.603	0.080	3.717	0.39
4^+_1	1.684	1	1.684	1
4^+_2	1.997	0.42	1.997	0.44
4^+_3	2.928	0.25	2.928	0.41
4^+_4	3.516		3.519	0.064
4^+_5			3.684	0.0080
4^+_6	3.958	0.10	3.958	0.24
4^+_7	4.113	0.14	4.008	0.056
4^+_8	(4.225)	(0.04)	4.631	0.0032
5^-_1	2.780	1	2.782	1
5^-_2	3.014	0.74	3.016	1.30
7^-_1	2.199	1	2.200	1
7^-_2	(2.865)	0.012	2.865	0.11
9^-_1	2.655	1	2.658	1

Energies are in MeV and $\sigma_{rel}(J^\pi_\alpha) = {}^{208}\mathrm{Pb(p, t)}^{206}\mathrm{Pb}(J^\pi_\alpha)/{}^{208}\mathrm{Pb(p, t)}^{206}\mathrm{Pb}(J^\pi_1)$. The cross sections were calculated using the code DWUCK [34]) with optical-model parameters as in ref. [12]).

of the total shell-model space determined by the single-particle levels in table 1. The matrix T_c could then be strongly non-hermitian, as discussed in the previous section. However, in all cases T_c was hermitian to within 25 keV.

The diagonalization of the metric matrix (7) provides the orthonormal basis elements $|m\rangle$ in eq. (8a). These elements are simply the eigenvectors of the metric matrix with eigenvalues different from zero [3]). In practice, however, we only consider those eigenvectors with eigenvalues λ larger than 0.1. This value is a few percent of the maximum value of $\lambda(\lambda_{max})$. For instance, for the state 0^+ one finds $\lambda_{max} = 5.6$, while $\lambda_{max}(2^+) = 4.4$, $\lambda_{max}(4^+) = 4.3$ and $\lambda_{max}(9^-) = 2.6$ (the smallest λ_{max} of our calculations).

In fig. 1 we present the calculated ^{204}Pb spectrum together with the experimental data as reported by Lanford for the ^{206}Pb(p, t) reactions [12]) or as given in ref. [38]) for those levels not observed in (p, t) reactions. Notice that all experimental levels

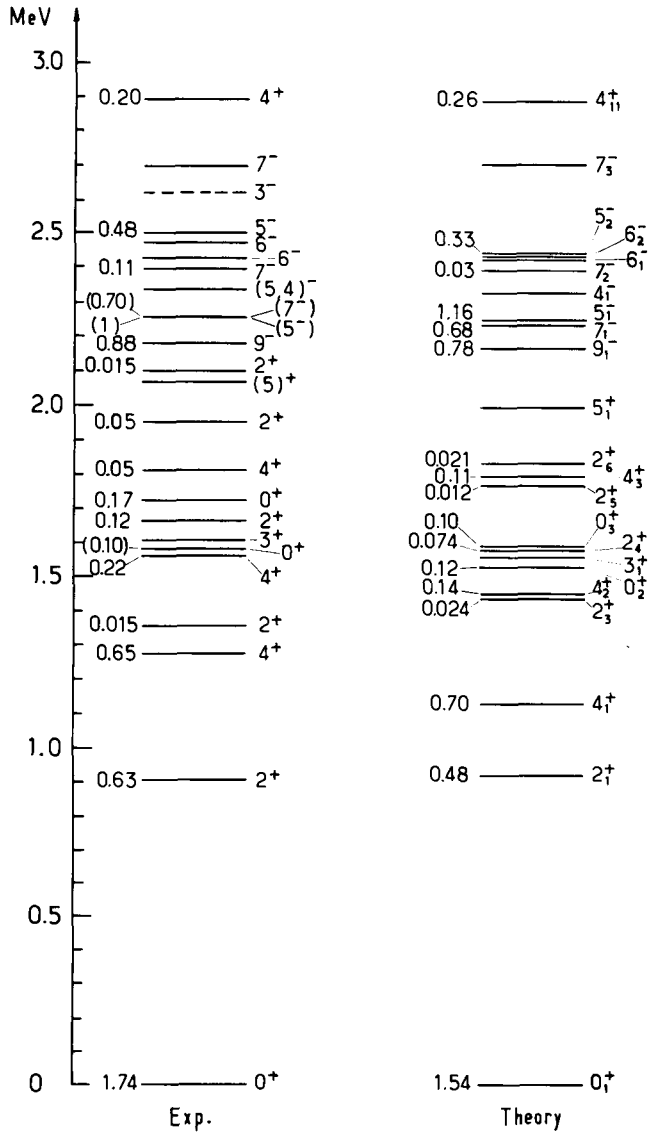

Fig. 1. Experimental [12, 38]) and calculated ^{204}Pb spectrum. The numbers to the left of the levels are the relative ^{206}Pb(p, t) cross sections (other details as in table 2). The dashed line is the octupole particle-hole vibration, which is not included in our calculations. All known experimental levels up to 2.9 MeV are included. The experimental (calculated) ground-state energy is 28.925 (28.865) MeV.

up to 2.9 MeV are given. Except for the 2^+ states with small (p, t) cross sections, the agreement between theory and experiment seems to be good. A feature which is particularly well reproduced is the order of the levels. The calculation confirms the near degeneracy of the 5^- and 7^- levels at 2.27 MeV as well as assigning the

value 4^- to the level at 2.34 MeV. The only level below 2.9 MeV not provided by this calculation is the 3^- at 2.63 MeV. This state is the octupole particle-hole vibration which is present at approximately the same energy in many of the Pb isotopes.

All the functions F, that appear in eq. (19), were provided by the calculation from the way we built the β-basis. The form factors that we thus calculated through eq. (19) coincided with those given by eq. (23). With these form factors we then evaluated the ^{206}Pb(p, t) cross sections using the code DWUCK [34]). In fig. 1 we give, as in ref. [12]), the ^{206}Pb(p, t)^{204}Pb(J^π) cross sections relative to the ^{208}Pb(p, t)^{206}Pb(J_1^π) cross sections. For each spin, only those levels with relative cross sections larger than $0.3\sigma_{rel}$(min), where σ_{rel}(min) is the minimum experimental relative cross section, are plotted in fig. 1. This procedure was followed only for the 0^+, 2^+ and 4^+ states. For these states the calculation predicts more levels than those observed experimentally (below 3 MeV). Generally, a very small form factor corresponds to the extra levels. This feature suggests that these levels may appear as a result of the truncations. In a complete calculation these states would correspond to eigenvalues $\lambda = 0$, i.e. they would be spurious states. Yet, there are states for which the form factors are not so small. A striking example is the calculated 2_2^+ state (predicted at 1.23 MeV) for which the form factor is, in absolute value, comparable to the one for the 2_1^+ state. But the phases are such that the corresponding relative cross section is equal to 0.0023.

From eq. (19) one can see that if there is a dominant value of the function F, say

$$F(\alpha\alpha_0; \beta) \sim C\delta_{\alpha\alpha'}, \tag{24a}$$

(note that $J_\alpha^\pi = J_\beta^\pi$) then

$$f(ij; \beta) \sim CX^*(ij; \alpha'). \tag{24b}$$

This feature helps in understanding the relation between the large relative cross sections in the ^{208}Pb(p, t) reactions (table 2) and those in the reaction ^{206}Pb(p, t) (fig. 1). In fact, if eq. (24) is valid one gets

$$\sigma_{rel}(\beta, J^\pi) = C^2\sigma_{rel}(\alpha', J^\pi), \tag{25}$$

where $\sigma_{rel}(\alpha'(\beta), J^\pi)$ is the ^{208,206}Pb(p, t) relative cross section. Thus, since C is

TABLE 3

(a) Projections $F(\alpha\alpha_0; \beta)$ [eqs. (10) and (19)] for $|\beta\rangle = |^{204}\text{Pb(g.s.)}\rangle$

α	ω_α	$F(\alpha\alpha_0; 0_1^+)$
0_1^+	0	1.10
0_2^+	1.167	0.54
0_3^+	2.315	0.11

(b) As in (a) for the states $|\beta\rangle = |^{204}\text{Pb}(4_1^+)\rangle$ and $|\beta\rangle = |^{204}\text{Pb}(4_2^+)\rangle$

α	ω_α	$F(\beta = 4_1^+)$	$F(\beta = 4_2^+)$
4_1^+	1.684	−0.86	−0.29
4_2^+	1.998	0.09	−0.84
4_3^+	2.929	−0.06	−0.09

α_0 labels the ^{206}Pb ground state. ω_α is the energy of the state ^{206}Pb(α) in MeV.

at most of order unity, larger values of $\sigma_{rel}(\beta, J^\pi)$ are necessarily associated with large values of $\sigma_{rel}(\alpha', J^\pi)$. For example, as seen in table 3b, $F(\alpha\alpha_0; 4_1^+) = -0.86$ corresponds to the ^{204}Pb(4_1^+) state for $\alpha = 4_1^+$, while $F \sim 0$ for the other values of α. Eq. (25) would then give $\sigma_{rel}(\beta = 4_1^+) = 0.74$ to be compared with $\sigma_{rel}(\beta = 4_1^+) = 0.70$ in fig. 1. Another interesting example is the $\beta = 4_2^+$ state. In this case, assuming that in eq. (24) $\alpha' = 4_2^+$ and $F = -0.84$ (as suggested by table 3) and using $\sigma_{rel}(\alpha' = 4_2^+) = 0.44$ (table 2), eq. (25) gives $\sigma_{rel}(\beta = 4_2^+) = 0.31$, to be compared with $\sigma_{rel}(\beta = 4_2^+) = 0.14$ in fig. 1. In this case the result is not as good as for the $\beta = 4_1^+$ state, but neither is the approximation (24). However, the general conclusion drawn from eq. (25) remains valid (at least qualitatively). Thus, for the ^{204}Pb(4_{11}^+) state the projection $F(4_3^+\alpha_0; \beta = 4_{11}^+)$ is large (-0.47) and since $\sigma_{rel}(\alpha = 4_3^+)$ is also large, one expects $\sigma_{rel}(\beta = 4_{11}^+)$ to be large, as indeed it is.

The relation for the two-particle transfer cross sections found above is a well-known feature resulting from the harmonic version of the pairing-vibrational model [13,16,36]. In this model one assumes that the operators $P^\dagger(\alpha)$ are boson creation operators. Therefore the elements (6) constitute an orthogonal basis and relations (24) and (25) are always valid. A typical two-phonon state in the pairing model is ^{204}Pb(g.s.), for which one has [36]

$$|^{204}\text{Pb(g.s.)}\rangle = N|\beta_1\rangle, \tag{26}$$

where $|\beta_1\rangle = (P^\dagger(\alpha_1 = 0_1^+)P^\dagger(\alpha_2 = 0_1^+))_{0^+}|0\rangle$ and $N = \sqrt{\frac{1}{2}}$. Eq. (24) then gives $C = \sqrt{2}$ (our calculation shows that $\langle\beta_1|\beta_1\rangle = 1.25$, as compared with $\sqrt{2}$). From eq. (25) one finally gets $\sigma_{rel}(^{204}\text{Pb(g.s.)}) = 2$. In this case we obtained, however, $\sigma_{rel} = 1.54$ (see fig. 1). Moreover, table 3a shows that the corresponding form factor has non-negligible contributions from states other than (26). This effect, due to the Pauli principle, has already been found and discussed in ref. [27]. The small value that we obtained for σ_{rel} as compared to the experimental data ($\sigma_{rel} = 1.74$) is because our calculation does not consider RPA correlations, which in this case seems to be important [27]. [This effect was not, however, found in ref. [36].]

The analysis of the six-particle spectrum carried out in subsect. 3.3 requires a description of the ^{204}Pb states in terms of as few basis states as possible. To do this, as well as to gain physical insight into the ^{204}Pb structure, we study the convergence of the ^{204}Pb eigenvectors as function of their basis components. As shown in the appendix, we expand those eigenvectors in an orthonormal basis following the Schmidt method. In table 4 we present the components of some β-states in the orthonormal basis and the corresponding convergence to the "shell-model" states. One sees in this table that indeed some β-states are well described within only one or two basis elements. As expected [36], the ^{204}Pb ground state is virtually the lowest basis vector (normalized). A similar property is found for the three-particle ground states in this nuclear region [9,10].

Besides the states shown in table 4, we also found the 2_1^+, 7_1^-, 7_2^- and 9_1^- states to be contained in the plane spanned by the first two basis vectors (6).

TABLE 4

Schmidt coordinates x and projections P_N [eq. (A.2)] as a function of the number N of basis vectors $|\alpha_1\alpha_2; \beta\rangle$

(a) $|\beta\rangle = |^{204}\text{Pb(g.s.)}\rangle$

N	$(\alpha_1\alpha_2)_\beta$	E_0	x	P_N
1	$(0_1^+0_1^+)_{0^+}$	28.218	0.98	0.96
2	$(0_1^+0_2^+)_{0^+}$	29.385	0.15	0.98
3	$(2_1^+2_1^+)_{0^+}$	29.824	−0.03	0.98

(b) $|\beta\rangle = |^{204}\text{Pb}(4_1^+)\rangle$ and $|\beta\rangle = |^{204}\text{Pb}(4_2^+)\rangle$

N	$(\alpha_1\alpha_2)_\beta$	E_0	$\beta = 4_1^+$		$\beta = 4_2^+$	
			x	P_N	x	P_N
1	$(2_1^+2_1^+)_{4^+}$	29.824	0.87	0.76	−0.16	0.03
2	$(0_1^+4_1^+)_{4^+}$	29.902	−0.49	1.00	−0.31	0.12
3	$(0_1^+4_2^+)_{4^+}$	30.216	0.01	1.00	−0.91	0.96

(c) $|\beta\rangle = |^{204}\text{Pb}(5_1^-)\rangle$ and $|\beta\rangle = |^{204}\text{Pb}(5_2^-)\rangle$

N	$(\alpha_1\alpha_2)_\beta$	E_0	$\beta = 5_1^-$		$\beta = 5_2^-$	
			x	P_N	x	P_N
1	$(0_1^+5_1^-)_{5^-}$	31.000	−0.86	0.74	−0.44	0.19
2	$(2_1^+7_1^-)_{5^-}$	31.221	0.38	0.88	−0.39	0.34
3	$(0_1^+5_2^-)_{5^-}$	31.234	0.29	0.97	−0.79	0.97

The energies $E_0 = \omega_{\alpha_1} + \omega_{\alpha_2}$ are in MeV.

Note that in table 4 the physical vectors are generally surrounded by some basis vectors. It would then be difficult to decide whether an eigenvector of the matrix (5) is spurious or not, even if in such a diagonalization spurious vectors are associated with zero-order energies [6]).

As one would expect, a feature emerging from tables 3 and 4 is that the overlap between the physical vectors and the basis vectors is smaller the greater the distance (in energy) between them. It is due to this property that the truncation procedure used here makes sense. In a standard shell-model calculation, basis vectors that are far apart in (zero-order) energy could have a similar importance in describing a physical vector. This is what happens, for instance, with the ground state of ^{210}Po, where the proton-proton normal pairing vibration plays an important role [25]). In methods which use correlated basis the pairing correlations are already included in the basis vectors. However, in a basis which is neither orthogonal nor normal

rather bizarre peculiarities may be present. In table 4b, for instance, the Schmidt coordinate, $x(0_1^+ 4_1^+ ; 4_1^+)$, is rather small (-0.49). Yet, the projection of the basis vector $|0_1^+ 4_1^+ ; 4^+\rangle$ on the physical vector $|\beta = 4_1^+\rangle$ is large ($F = -0.86$, table 3). One may think that this feature is due to the criterion used to choose the orthonormal basis. In fact, as seen in fig. 2, a physical state can coincide with a basis vector,

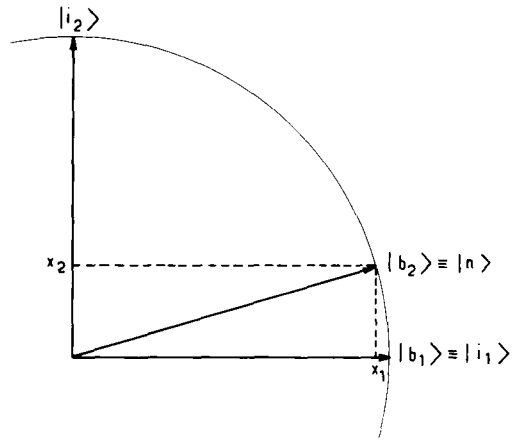

Fig. 2. The basis vector $|b_2\rangle$ coincides with the physical vector $|n\rangle$, yet the corresponding Schmidt coordinate x_2 is small. In this figure the basis vectors $|b_i\rangle$ are supposed to be normalized. The vectors $|i_1\rangle$ and $|i_2\rangle$ are the Schmidt unit vectors.

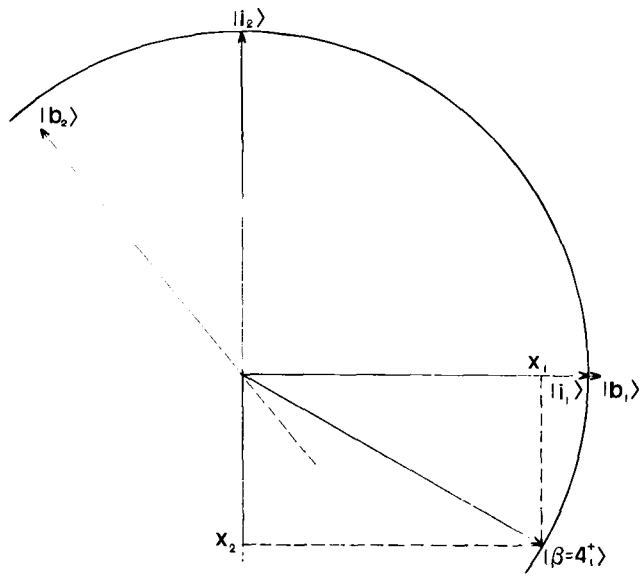

Fig. 3. The calculated state $|\beta\rangle = |^{204}\mathrm{Pb}(4_1^+)\rangle$ projected in the plane spanned by the basis vectors $|b_1\rangle = |2_1^+ 2_1^+ ; 4^+\rangle$, $|b_2\rangle = |0_1^+ 4_1^+ ; 4^+\rangle$. Unlike the $|\beta = 4_{1_1}^+\rangle$ state of fig. 4, in this case the physical vector is contained in the figure plane and its projection $|\beta = 4_1^+\rangle_p$ coincides with itself. The circle's radius is unity and $|i_1\rangle$ and $|i_2\rangle$ are the unit Schmidt vectors.

retaining a small coordinate in the Schmidt axis corresponding to that basis vector. This shows that although it is instructive to have the decomposition of a physical state into its orthonormal components, one has to be cautious. In case of doubt it is better to draw a diagram like the one in fig. 2. Thus, in fig. 3 we see that what happens with the vector $|\beta = 4_1^+\rangle$ is that it is somewhat closer to the basis vector $|b_2\rangle$ than to $|b_1\rangle$. On top of that, the norms of the basis vectors are $\sqrt{(\langle b_1|b_1\rangle)} = 1.04$, while $\sqrt{(\langle b_2|b_2\rangle)} = 0.93$.

The $|\beta = 4_{11}^+\rangle$ state, which in terms of its Schmidt coordinates seems to be rather mixed, could yet be close to a basis vector, as the vector $|n\rangle$ in fig. 2. This possibility is suggested by the fact that the $|^{204}\text{Pb}(4_{11}^+)\rangle$ state has a large (p, t) cross section (fig. 1). One would then think that the basis vector $|b_1\rangle = |0_1^+ 4_3^+; 4^+\rangle$ is more important in describing that state (as discussed above) than our Schmidt decomposition implies. To decide upon this point (which is very important for our calculation of the ^{202}Pb spectrum) we draw several diagrams like the one in fig. 3. In each case we chose a plane spanned by two of our basis vectors. In fig. 4 we show a plane onto

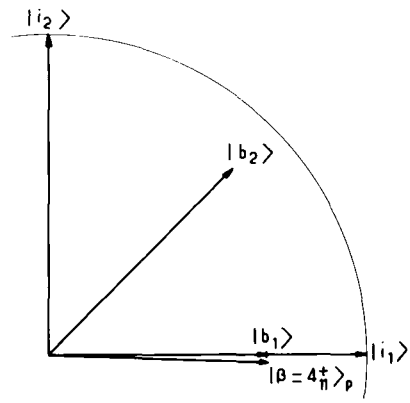

Fig. 4. As fig. 3 for the vector $|\beta\rangle = |^{204}\text{Pb}(4_{11}^+)\rangle$. The basis vectors are $|b_1\rangle = |0_1^+ 4_3^+; 4^+\rangle$, $|b_2\rangle = |0_2^+ 4_3^+; 4^+\rangle$.

which the vector $|\beta = 4_{11}^+\rangle$ has one of the largest projections. Although in this figure the vectors $|4_{11}^+\rangle$ and $|b_1\rangle$ seems to be close, the angle between them is 46.3° and the projection of $|4_{11}^+\rangle$ onto that plane ($|\beta = 4_{11}^+\rangle_p$) is therefore small. One reason why the vector $|b_1\rangle$ is not as important as one would expect is that its norm is small. From a physical point of view, this property means that $|b_1\rangle$ is blocked by the Pauli principle. Indeed, the vector $|\alpha = 4_3^+\rangle$ is virtually the $|(p_{\frac{1}{2}} f_{\frac{7}{2}})_{4^+}\rangle$ state, and the main component of the vector $|\alpha = 0_1^+\rangle$ is $|(p_{\frac{1}{2}})_{0^+}^2\rangle$. This analysis brings us to the conclusion that it is not the energy criterion used here to choose the β-basis which fails to give a "pure" description of the state $|\beta = 4_{11}^+\rangle$. Rather, it is both because the vector $|b_1\rangle$ is blocked and because many other basis states are close to it, that the physical vector is spread into many components.

After one has a clear idea about which β-basis vectors are important in the description of the β-vector, one can attempt to calculate the matrix $\tilde{T}$ in as small as possible a β-basis. In this case, as with the large β-basis, one may encounter strongly non-hermitian T_c matrices. However, for the $\beta = 4^+$ states and with the 2-dimensional β-basis $|b_1\rangle = |0_1^+ 4_1^+; 4^+\rangle$, $|b_2\rangle = |0_1^+ 4_2^+; 4\rangle$ (which is enough to describe the vector $|\beta = 4_2^+\rangle$, see table 4b) one finds the matrix T_c to be hermitian, with the non-diagonal matrix element equal to -0.128 MeV. But this case is rather exceptional. In general, the matrix T_c is hermitian only within 100 keV.

To be sure that a calculation within a small β-basis (SB) is reasonable we compared the calculated projections F with those values obtained with the large β-basis, which we call from now on "shell-model" values. In table 5 we present some states

TABLE 5

Projections $F(\alpha_1\alpha_2; \beta)$ [eq. (10)] for some β-states calculated within the basis composed of the elements in the column headed "β-basis"

β-state	β-basis	SB	SM
0_1^+	$\|0_1^+ 0_1^+; 0^+\rangle$	1.10	1.10
2_1^+	$\|0_1^+ 2_1^+; 2^+\rangle$	0.62	0.60
	$\|2_1^+ 2_1^+; 2^+\rangle$	−0.77	−0.72
4_1^+	$\|0_1^+ 4_1^+; 4^+\rangle$	−0.83	−0.86
	$\|2_1^+ 2_1^+; 4^+\rangle$	0.95	0.90
4_2^+	$\|0_1^+ 4_1^+; 4^+\rangle$	−0.31	−0.29
	$\|0_1^+ 4_2^+; 4^+\rangle$	−0.82	−0.84
	$\|2_1^+ 2_1^+; 4^+\rangle$	−0.16	−0.18
5_1^-	$\|0_1^+ 5_1^-; 5^-\rangle$	−0.87	−0.83
	$\|2_1^+ 7_1^-; 5^-\rangle$	0.52	0.50
	$\|0_1^+ 5_2^-; 5^-\rangle$	0.38	0.42

The results obtained with the small basis (SB) are given together with those obtained with the "shell-model" (SM), i.e. the large β-basis.

calculated within the small β-basis together with the corresponding shell-model description. Although the results shown in table 5 are very good, they deal only with the β wave functions. The β-energies are not always as good. The $|^{204}\text{Pb(g.s.)}\rangle$ state has, in the 1-dimensional basis of table 5, energy $E_{SB} = 28.740$ MeV (as compared with the shell-model value $E_{SM} = 28.865$ MeV). Other examples (energies in MeV) are:

$$E_{SB}(4_1^+) = 29.797, \quad E_{SM} = 29.988, \quad E_{SB}(4_2^+) = 30.375, \quad E_{SM} = 30.315,$$
$$E_{SB}(5_1^-) = 31.001, \quad E_{SM} = 31.123.$$

Since the SB projections, F, are in good agreement with the corresponding shell-model projections, one may consider that the main effect of the drastic truncation done within the small β-basis is to renormalize the β-energies. Moreover, if one increases the dimensions of the β-basis in table 5 by one or two units, one obtains great improvements. Thus, $E_{SB}(0_1^+) = 28.852$ MeV for a 2-dimensional β-basis. For the state $\beta = 4_1^+$ one obtains, with dimension 4, $E_{SB}(4_1^+) = 30.066$ and similarly for the other states. In all cases the values of F reported in table 5 remain without change.

With the SB wave functions corresponding to table 5 we calculated the two-particle transfer form factor according to eq. (23). In general one obtains the same form factors as those provided by the shell model. However, there are a few states, like $|\beta = 2_1^+\rangle$, for which differences (up to 30 %) appear. Again in these cases, the results are improved by increasing slightly the dimensions of the β-basis.

For the next step, i.e. the calculation of the ^{202}Pb spectrum, the important SB quantities are those shown in table 5, which in all cases are in excellent agreement with the corresponding shell-model quantities.

3.3. γ-STATES: THE NUCLEUS ^{202}Pb

The third and final step of our method is to calculate the six-particle system, i.e. the γ-states of sect. 2. The first point to study is how to choose appropriate α- and β-states to form the γ-basis,

$$\{|\alpha\beta; \gamma\rangle\} = \{(P^\dagger(\alpha)P^\dagger(\beta))_\gamma|0\rangle\}, \tag{27}$$

used in (14) to describe the six-particle γ-states. As for the four-particle system, once the γ-basis is chosen one calculates the matrix T_c from eq. (8a), where M is now the matrix (11). Finally the γ-eigenvectors are provided by the diagonalization of the hermitian matrix $\tilde{T}$ [eq. (8b)]. Regarding the truncation procedure and the attached loss of hermiticity of the matrix T, the analysis done for the four-particle case remains valid.

If one chooses directly a rather large number of low-lying α- and β-states, as calculated with the large β-basis, and applies eqs. (11) and (12) without further analysis one obtains results as reported in ref. [11]). A large number of γ-states are provided by the calculation; much more than observed experimentally. Moreover, the states with largest (p, t) cross sections are usually not the lowest ones, as one would expect. As for the four-particle system, one may think that many of these states result from the truncation procedure. In a very large γ-basis this effect would loose its importance. However, the calculation of the overlap matrix (12) is very time consuming and a complete calculation within a large γ-basis becomes prohibitive. The real problem with eq. (12) lies in the last term of the r.h.s. The intermediate four-particle state index β and the α-states α_4 and α_5 may easily run over a large range of values. For instance, if the state α_2 in the γ-basis is the state $|^{206}\text{Pb}(7_1^-)\rangle$

and the intermediate state α_4 is $|^{206}\mathrm{Pb}(4_1^+)\rangle$, β takes the values $3^- \leqq \beta \leqq 11^-$. One must then calculate a large number of four-particle states. This problem can be eased if one replaces the four-particle metric matrix in eq. (13) by its analytic expression (7). In this case the β-state index β is replaced by an angular momentum index only. Still, the CPU time taken to calculate a γ-state matrix element T_c is typically about 3 s in a CDC-6400 machine. This CPU time is about 15 times larger than the corresponding value for the four-particle system.

The way we found of overcoming this problem, is to use only pure β-states in the γ-basis, such as those in table 5. One then finds that the amplitude Y in eq. (12) greatly reduces the number of intermediate states α_3 and α_4 and, therefore, the number of intermediate states β. From the viewpoint of our calculation, this was the most important reason for studying the β-states within a small β-basis: to find the minimum number of coordinates necessary to describe the β-vector. Since the projections F are well given by our SB calculation (table 5) we let the values of F in eq. (12) to be those obtained within the shell-model calculation. Thus, although the index α_5 in eq. (12) is not limited by our choice of representation for the vector $|\beta_1\rangle$, the corresponding values of F are provided by the large β-basis calculation.

In the procedure outlined above the β-vectors entering in the γ-basis (27) are supposed to be pure states. In fact, we saw in the calculation of the four-particle system that, at least for the analysis of (p, t) reactions, only α-states with a very definite structure were relevant. Namely, those states to which rather large (p, t) cross sections correspond. This feature [which underlies the pairing-vibration model [16])] suggests that for the γ-states only a γ-basis built upon those relevant α- and β-states (the "collective" states of the pairing model) will be important. Of all the "collective" states, only the $|\beta = 4_{11}^+\rangle$ state is not "pure". We thus described this state in a large enough β-basis to obtain projections F close to the shell-model values.

Although the calculations done within the smallest possible β-basis (as in table 5) did not always give the right β-state energies, we speculated in the last subsection that the difference was only a renormalization effect. Moreover, since even the shell-model values did not fully agree with the experimental energies, we simply take for our "pure" states the experimental β-energies. A more general justification of this procedure was given at the beginning of this section.

We formed our γ-basis taking the same α-states used to calculate the shell-model spectrum of fig. 1. The β-states that we took were the following: 0_1^+, 2_1^+, 4_1^+, 4_2^+, 4_{11}^+, 5_1^-, 5_2^-, 7_1^-, 7_2^-, 9_1^-. To calculate the matrix $\tilde{T}$ we profited from the experience gained in the analysis of the four-particle system. We thus reduced the dimensions of the γ-basis to the first 20 elements, except for the $|\gamma = 0_1^+\rangle$ state, for which we used a 4-dimensional γ-basis. In all cases the matrix T_c was hermitian to within 100 keV, as for the four-particle case. Finally, the calculation of the form factor was performed using the method (b) of subsect. 2.2.

In table 6 we present the calculated ^{202}Pb spectrum together with the corre-

TABLE 6

Experimental [12]) and theoretical ^{202}Pb energies and relative ^{204}Pb(p, t) cross sections

Experiment			Theory		
J^π	E (MeV)	σ_{rel}	J^π	E (MeV)	σ_{rel}
0_1^+	44.112	2.31	0_1^+	44.109	1.89
2_1^+	45.073	0.56	2_1^+	45.015	0.46
(2_2^+)	45.696	0.026	2_5^+	45.647	0.034
			2_6^+	46.086	0.058
4_1^+	45.495	0.48	4_1^+	45.432	0.56
4_2^+	45.735	0.090	4_3^+	45.679	0.027
4_3^+	46.027	0.067			
4_4^+	46.628	0.086			
4_5^+	46.778	0.115	4_6^+	46.695	0.069
5_1^-	46.152	1.28	5_1^-	46.202	1.59
			5_2^-	46.511	0.045
			7_1^-	46.363	0.040
			7_2^-	46.751	0.32
9_1^-	46.284	0.93	9_1^-	46.310	0.62

Only calculated values of $\sigma_{rel} \geqslant 0.02$ are given. Energies relative to the ^{208}Pb core. Other details as in table 2.

sponding experimental data. Only levels up to 2.7 MeV of excitation energy [with respect to ^{202}Pb(g.s.)] are given. The agreement between theory and experiment is excellent for those states with a large ^{204}Pb(p, t) cross section.

The agreement to within a few keV between the experimental and theoretical ^{202}Pb(g.s.) energies does not seem to be accidental. As a function of the dimensions (d) the energy (in MeV) changes as follows:

$$E(d = 1) = 44.450, \quad E(d = 2) = 44.173, \quad E(d = 3) = 44.180, \quad E(d = 4) = 44.109.$$

Moreover, the form factor does not change for $d \geqq 2$, but for $d = 1$ one obtains $\sigma_{rel}(\gamma = 0_1^+) = 2.19$, much closer to the experimental value than that obtained with $d > 1$. Although here (as in ^{204}Pb) the RPA ground-state correlations, which we ignored, may play some role, it was found in ref. [36]) that a (schematic) ^{202}Pb(g.s.) TDA wave function provides the same σ_{rel} as the corresponding BCS wave function. Even more, in that paper ^{202}Pb(g.s.) was found to be very pure. On the other hand, we have seen that the vector $|^{204}\text{Pb(g.s.)}\rangle$ is contained in a 1-dimensional space, even when the corresponding energy is only given utilizing a 2-dimensional basis, exactly as in the case of ^{202}Pb(g.s.) analysed here. We may thus think that the differences encountered between $d = 1$ and $d > 1$ are due to the limitations imposed by the non-orthogonal basis. This supposition is supported by the fact that the angle θ between the lowest two basis vectors, $|\gamma_1\rangle = |0_1^+ 0_1^+; 0^+\rangle$ and $|\gamma_2\rangle = |0_2^+ 0_1^+; 0^+\rangle$ [notation as in eq. (27)], is such that $\cos\theta = 0.95$, i.e. both vectors are

nearly parallel. Finally, while $\langle\gamma_1|\gamma_1\rangle = 1.55$ (the pairing-model predicts $\langle\gamma_1|\gamma_1\rangle = \sqrt{6} = 2.45$) one finds $\langle\gamma_2|\gamma_2\rangle = 0.657$, i.e. the state $|\gamma_2\rangle$ is much blocked by the Pauli principle. Therefore, it does not seem reasonable to consider that the state $|\gamma_2\rangle$ can have any real physical importance, and the state ^{202}Pb(0_1^+) seems to be a pure $|^{206}\text{Pb(g.s.)} \otimes {}^{204}\text{Pb(g.s.)}\rangle$ (normalized) state.

One reason why the state $|^{202}\text{Pb(g.s.)}\rangle$ [as well as $|^{204}\text{Pb(g.s.)}\rangle$ and other ground states in the lead region [9,10])] is so pure is that the first basis vector is isolated (in energy) from the rest of the basis. This property is not present in the other states of table 6. An interesting example is $|\gamma = 2_1^+\rangle$ which can be described in the 2-dimensional basis

$$|\gamma_1\rangle = |2_1^+ 0_1^+; 2^+\rangle, \qquad |\gamma_2\rangle = |0_1^+ 2_1^+; 2^+\rangle. \tag{28}$$

Within this γ-basis one obtains practically the same $|\gamma = 2_1^+\rangle$ level as the corresponding one in the 20-dimensional basis of table 6. The zero-order energy associated with (28) is $E(\gamma_1) = 43.838$ MeV, $E(\gamma_2) = 43.933$ MeV. According to the analysis of subsect. 3.2, one would expect that the two-particle transfer reaction proceeds via the basis element $|\gamma_1\rangle$. However one finds that $\langle\gamma_1|\gamma_1\rangle = 0.28$, i.e. the basis element is very much blocked by the Pauli principle. The reason why the Pauli principle is so effective in this case is that at least one of the two particles in the α-state 2_1^+ spends 93 % of the time either in the $p_{\frac{1}{2}}$ or $p_{\frac{3}{2}}$ shells, both of which are very much occupied by the four particles in the β-state 0_1^+. In the case of the basis element $|\gamma_2\rangle$, instead, the two particles in the α-state 0_1^+ occupy these single-particle shells for only 68 % of the time.

The rest of the levels in table 6 are also strongly influenced by the Pauli principle. For instance, the reason why only the 4_1^+ level is highly excited by the (p, t) reaction (in contrast to the 4^+ states in ^{206}Pb and ^{204}Pb) is that the important basis vectors $|\gamma_1\rangle = |4_2^+ 0_1^+; 4^+\rangle$ and $|\gamma_2\rangle = |4_3^+ 0_1^+; 4^+\rangle$ have the norms (square) $\langle\gamma_1|\gamma_1\rangle = 0.63$ and $\langle\gamma_2|\gamma_2\rangle = 0.36$.

Finally, we repeated our calculations making the "quasi-boson" approximation of dropping the last term in eq. (12). We found that it is a good approximation for the $|\gamma = 0^+\rangle$ states but fails for the other γ-states.

4. Summary and conclusions

In this paper a method is presented of solving the six-particle system outside closed-shell cores in several steps. First the two-particle system is solved. In this step a good knowledge of the nucleon-nucleon interaction is supposed or, alternatively, the two-particle energies and wave-function amplitudes are supposed to be extracted from experiment [26]). Once a good description of the two-particle (α) states is found one proceeds to the second step. In this step, the four-particle system is solved within a basis formed by vector coupling the α-states previously evalu-

ated [3,4,6]). The two-particle interaction matrix elements are then replaced by the corresponding two-particle energies and wave functions [6]). The dynamical matrix so obtained is very similar to the corresponding overlap matrix among the basis vectors (metric matrix). Both matrices depend only on one- and two-particle quantities and the formalism turns out to be rather simple and effective. Once the four-particle (β) states are calculated one proceeds to the third and last step. In this step the six-particle system is solved within a basis formed by vector coupling the α- and β-states previously evaluated. The corresponding dynamical and metric matrices depends only upon two- and four-particle quantities. Although in this case both matrices are not as similar to each other as for the β-states, the formalism is still simple. Within an example, we showed that this method exactly reproduces the shell-model results. In fact, this method (as all methods that use a correlated basis) allows one to solve the shell-model equations in a convenient representation. Therefore, drastic truncations of the basis are possible and the physical vectors may be described in terms of a few basis vectors.

We applied the formalism to the lead region. We thus first calculated the ^{204}Pb spectrum using the ^{206}Pb energies and wave functions as calculated by Blomqvist [31]). The agreement between theory and experiment is good. We found that those ^{204}Pb states highly excited in the ^{206}Pb(p, t) reaction are closely related to some states in ^{206}Pb; precisely those which are highly excited in the ^{208}Pb(p, t) reaction. Thus, a microscopic description of the pairing-vibration phonons [16]) is given. However, in the pairing-vibration model one usually assumes that the "collective" states are only the lowest states of each spin and parity. It is for these states that all components of the wave functions contribute in phase to the two-particle transfer cross section [41]). We have found that the concept of "collective states" (pairing bosons) may be enlarged to include all α-states with a large (p, t) cross section. The role of the Pauli principle limiting the validity of both the harmonic pairing-vibration model and the concept of pairing bosons was attested. It was thus found that some multiphonon states [like the experimental ^{204}Pb(4_4^+) state, at 2.9 MeV of excitation energy] are strongly hindered by the Pauli principle. They cannot be described in term of a few basis vectors. But the other β-states reached in the ^{206}Pb(p, t) reaction are well described within a very small (less than 4-dimensional) basis, although the corresponding shell-model dimensions are always, at least, several hundred. Using this "pure" description of the β- and the α-states evaluated in the first step, we calculated the ^{202}Pb spectrum. The agreement between theory and experiment is very good for the states with a relatively large ^{204}Pb(p, t) cross section. It is found that some pairing multiphonon states, expected from the pairing collectivity of the α- and β-constituents, are completely blocked by the Pauli principle. Although the shell-model dimensions for describing the ^{202}Pb states are always of the order of several thousand, we found that those ^{202}Pb levels experimentally observed in the (p, t) reaction are contained in subspaces spanned by very few basis vectors. We conclude that the ground states of the Pb isotopes analysed here are particularly

well described within a one-dimensional vector-coupled basis consisting of monopole pairing-vibrational states. The states of multipolarity different from zero, however, may strongly feel the blocking induced by the Pauli principle and relevant collective (multipole-pairing) configurations have not the importance that one would attach to them within the harmonic pairing model. In spite of these (expected) limitations, the pairing model remains a very good guide for analysing two-particle transfer reactions. Thus, all states highly excited in the ^{204}Pb(p, t) reactions are of a pairing model character.

We are indebted to J. Blomqvist for providing us with and allowing us to freely publish his ^{206}Pb wave functions [31]). Discussions with Y. Abgrall, J. Blomqvist, C. Meyers and A. Zuker are greatfully acknowledged.

Appendix

We assume that the ^{204}Pb spectrum obtained with the large β-basis (fig. 1) is the shell-model spectrum. To see whether the (shell-model) β-states in fig. 1 can be described, within our representation, in terms of a few basis vectors, we rewrite these states in an orthonormal basis. This basis is constructed, using the Schmidt procedure [39]), from the original β-basis according to the energy criterion; i.e. the first orthonormal (Schmidt) vector $|i = 1\rangle$ is the lowest vector (6) (normalized), the second Schmidt vector $|i = 2\rangle$ is constructed from the first one and the second lowest state (6) and so on. In the step N of this procedure one has,

$$|\beta; \mathrm{SB}\rangle = \sum_{i=1}^{N} x(i; \beta)|i\rangle, \tag{A.1}$$

where $|\beta; \mathrm{SB}\rangle$ is the projection of the vector $|\beta\rangle$ onto the subspace spanned by the "small basis" (SB) composed by the first N Schmidt vectors. Therefore, the overlap between the shell-model β-state and its projection onto the small subspace is

$$P_N = \sum_{i=1}^{N} x^2(i; \beta). \tag{A.2}$$

An important feature of this procedure is that the coordinates x give a clear idea of which are the relevant states (6) to describe the physical vectors, as seen in table 4.

References

1) G. Do Dang, G. J. Dreiss, R. M. Dreizler, A. Klein and Chi-Shiang Wu, Nucl. Phys. **A114** (1968) 481; A. Arima and I. Hamamoto, Ann. Rev. Nucl. Sci. **21** (1971) 55; and references therein
2) J. D. Vergados, Phys. Lett. **34B** (1971) 458; S. K. M. Wong and A. P. Zuker, Phys. Lett. **36B** (1971) 437
3) C. M. Ko, T. T. S. Kuo and J. B. McGrory, Phys. Rev. **C8** (1973) 2379

4) W. W. True and C. M. Ma, Phys. Rev. **C9** (1974) 2275
5) P. Ring and P. Schuck, Z. Phys. **269** (1974) 323; Phys. Rev. **C16** (1977) 801
6) P. Schuck, R. Wittmann and P. Ring, Nuovo Cim. Lett. **17** (1976) 107;
P. Schuck, Z. Phys. **A279** (1976) 31
7) D. R. Bès, G. G. Dussel, R. A. Broglia, B. Mottelson and R. Liotta, Phys. Lett. **52B** (1974) 253
8) P. F. Bortignon, R. A. Broglia, D. R. Bès and R. Liotta, Phys. Reports **30C** (1977) 305
9) R. J. Liotta, C. Pomar and B. Silvestre-Brac, Symp. on pure and applied nuclear physics, Stockholm 1978; Lett. Nuovo Cim. **27** (1980) 100
10) J. P. Boisson, B. Silvestre-Brac and R. J. Liotta, Nucl. Phys. **A330** (1979) 307
11) C. Pomar and R. J. Liotta, Phys. Lett. **92B** (1980) 229
12) W. A. Lanford, Phys. Rev. **C16** (1977) 988
13) D. R. Bès, R. A. Broglia, O. Hansen and O. Nathan, Phys. Reports **34C** (1977) 1
14) A. P. Zuker, Int. Conf. on nuclear structure and spectroscopy, Invited talks, Amsterdam, Sept., 1974
15) D. H. Gloeckner and F. J. D. Serduke, Nucl. Phys. **A220** (1974) 477; and references therein
16) A. Bohr and B. R. Mottelson, Ann. Rev. Nucl. Sc. **23** (1973) 363;
D. R. Bès and R. A. Broglia, Nucl. Phys. **80** (1966) 289
17) R. A. Broglia, O. Hansen and C. Riedel, Advances in nuclear physics, ed. M. Baranger and E. Vogt, Vol. 6 (Plenum, NY, 1973) p. 287
18) A. Bohr and B. R. Mottelson, Nuclear structure, vol. II (Benjamin, New-York, 1975)
19) R. A. Broglia, R. Liotta, B. S. Nilsson and A. Winther, Phys. Reports **29C** (1977) 291
20) I. Tonozuka and A. Arima, Nucl. Phys. **A323** (1979) 45
21) P. Federman and S. Pittel, Phys. Rev. **C20** (1979) 820
22) R. Vennink and P. W. M. Glaudemans, Z. Phys. **A294** (1980) 241
23) E. Pasquini, CRN/PT 76-14, Ph.D. Thesis, Strasbourg (1976)
24) A. Poves, E. Pasquini and A. P. Zuker, Phys. Lett. **82B** (1979) 319;
A. Cortes and A. P. Zuker, Phys. Lett. **84B** (1979) 25
25) F. Janouch and R. J. Liotta, Nucl. Phys. **A334** (1980) 427
26) N. Auerbach and I. Talmi, Nucl. Phys. **64** (1965) 458;
J. B. Ball, J. B. McGrory and J. S. Larsen, Phys. Lett. **41B** (1972) 581; and references therein
27) J. B. McGrory and T. T. S. Kuo, Nucl. Phys. **A247** (1975) 238
28) J. Blomqvist, I. Bergström, C. J. Herrlander, C. G. Linden and K. Wikström, Phys. Rev. Lett. **38** (1977) 534
29) C. G. Linden, I. Bergström, J. Blomqvist and C. Roulet, Z. Phys. **A284** (1978) 217
30) C. G. Linden, I. Bergström, J. Blomqvist, K. G. Rensfelt and B. Fant, Z. Phys. **A277** (1976) 273
31) J. Blomqvist, unpublished
32) T. T. S. Kuo and G. H. Herling, Naval Research Laboratory report 2258 (Washington, DC, 1971); G. Herling and T. T. S. Kuo, Nucl. Phys. **A181** (1972) 113
33) W. A. Lanford and J. B. McGrory, Phys. Lett. **45B** (1973) 238
34) P. D. Kunz, unpublished
35) E. R. Flynn, G. J. Igo and R. A. Broglia, Phys. Lett. **41B** (1972) 397
36) E. R. Flynn, R. A. Broglia, R. Liotta and B. S. Nilsson, Nucl. Phys. **A221** (1974) 509; **A343** (1980) 24
37) R. J. Liotta, Proc. Int. School on nuclear physics. Invited lectures, Predeal, Rumania, 1978
38) M. R. Schmorac, Nucl. Data Sheets **27** (1979) 581
39) P. M. Morse and H. Feshbach, Methods of theoretical physics, vol. I (McGraw-Hill, NY, 1953)
40) M. P. Webb, Nucl. Data Sheets, Vol. **26** (1976) 145
41) D. R. Bès and R. A. Broglia, Phys. Rev. **C3** (1971) 2349